WYLE LABORATORIES
TESTING DIVISION, HUNTSVILLE FACILITY

research report

WYLE LABORATORIES RESEARCH STAFF
Report WR 66-29

# A TECHNIQUE FOR THE DYNAMIC CALIBRATION OF HOT WIRE ANEMOMETERS

by

R. C. Potter

Submitted under NASA Contract No. NAS8-11312

Prepared by R.C. Potter
R. C. Potter

Approved by
L. C. Sutherland
Research Operations Manager

Approved by Kenneth McK. Eldred
Kenneth McK. Eldred
Director of Research

Date July, 1966

COPY NO. 32

## SUMMARY

A technique for dynamically calibrating hot wire anemometers is examined. The wire is mounted on the end of a cantilever beam, which is driven at its natural frequency of vibration by an electro-mechanical shaker. The wire is positioned in the laminar core of a subsonic cold jet. The output signal is compared to a value calculated from the static calibration of the wire, when the wire is held still in a steady air flow, and the measured frequency and displacement of the wire. A statistical analysis of the results, including digital calculation of the probability function, and the form, skewness, and flatness factors of the output signals is completed. Very little difference between the two sets of results is determined for the limited range of frequencies and velocity covered here. However, at the lowest mean velocity, 92 fps, and the highest frequency, 245 cps, the output voltage shows a more sharply peaked signal than obtained for the calculated values from the static calibration. It is suggested that at low mean velocities, in rarefied atmospheres, and in supersonic flows, the inertia of the viscous flow field over the wire could become significant and cause the convective heat transfer process to change from the static calibration example. Thus, the dynamic calibration technique becomes extremely useful.

TABLE OF CONTENTS

## LIST OF FIGURES

LIST OF TABLES

## 1.0 INTRODUCTION

The calibration of hot wire anemometers, used for measurements of fluctuating velocity components, is normally based on measurements made in a steady flow. The wires are positioned in a smooth steady air stream, such as the core of a jet, and the resultant mean voltage output is compared to the velocity measured with a pitot-static tube combination. Then the wire is used in a turbulent flow to measure fluctuating velocity components, rather than the mean velocities, which are more easily measured with other instruments anyway. When the wire is placed in the turbulent flow, it is assumed to behave exactly as it does in the steady flow. The rapidly changing velocity is considered as just moving the operating conditions of the wire and amplifier along the steady flow calibration curve. Figure 1 illustrates this point. This figure shows a typical calibration curve for a hot wire anemometer. The voltage output E increases as the steady air velocity over the wire V increases, but the sensitivity of the system decreases with increasing air velocity, so the calibration is not a linear curve. The heat balance of a constant temperature hot wire anemometer is complex, involving the addition of heat by the electric current equaling the heat convected away. The total resistance of the wire must remain essentially constant, and the process will be complicated by the heat flow to the supports and the resulting temperature profile across the wire. A full discussion of the operation of hot wire anemometers is given in References 1 to 5, and details of specific equipment and techniques for operation and construction are given in References 6 to 9.

Returning to Figure 1, the application of a fluctuating velocity is always assumed to cause a fluctuating voltage directly derived from the static calibration curve. In the measure of turbulent intensities, this static calibration curve is linearized by a suitable function generator, and the rms level of the fluctuating voltage output measured, and compared to the mean dc voltage. However, analysis of the operation of the wire has shown that the cooling process is very complicated, and more involved when the wire considered has a finite length (References 10 and 11). Davis and Fisher in Reference 10 analyze the varying temperature profile across a wire in a fluctuating flow, an effect which still occurs for a constant temperature hot wire anemometer. Corrsin in Reference 11 discusses the effect of yawing a wire to the air stream, and the traditionally used cosine law, assuming that the wire only reacts to the normal velocity component, is shown to be incorrect for short lengths. The effect of yawing the wire is to cause the temperature profile across the wire to become unsymmetrical, as also discussed by Davies and Fisher in Reference 10.

When a wire is placed in a turbulent flow, where the local velocity is changing rapidly, both in magnitude and direction, it is possible that significant differences from the static flow case could occur. The velocity direction will remain reasonably consistent for a normal turbulent flow, but the local velocity will be changing. The dynamic response of the system will depend upon certain time constants associated with the thermal inertia of the wire, the thermal inertia of the air field, and the viscous convective cooling of the wire by the changing air flow. The thermal inertia terms of the wire, concerning the change in temperature profile and the change in radial heat conduction

as the heat flow through the system changes, will be generally insignificant for the constant temperature system, and especially so at low frequencies of velocity fluctuation. The thermal inertia of the gas will also be considered small, but the viscous field effects could cause errors. This could mean that the convective cooling process is altered momentarily from the equivalent static velocity case. Then the wire will not follow the assumed performance, Example 1, shown in Figure 1, but could perhaps follow the path of the possible performance of Example 2.

The experiment reported here is concerned with a technique for dynamic calibration of the hot wires and will examine these points. It is based on using a steady flow and moving the wire in a known fashion, to create a known fluctuating flow. The next sections of this report describe the apparatus used, present details, and analysis of the values measured, and give the conclusions.

## 2.0 DESCRIPTION OF THE EXPERIMENT

The hot wire anemometer was a constant temperature system using a tungsten wire 0.060 in. long and 0.00025 in. diameter. The wire was placed across the tips of two steel sewing needles, which were bonded to, and insulated from, a six inch steel rule. This rule was bonded to either one or two other rules and then cut to different lengths. The rule was mounted to the head of a 25 pound electro-mechanical shaker, and was arranged to be vertical, with the anemometer wire just in the core of a 2 in. diameter subsonic air jet (see Figure 2). The jet speed was kept constant and measured with a pitot-static tube, and the rule was vibrated at its natural frequency. The wire was then at the end of a vibrating cantilever beam and thus has a simple harmonic motion in the mean jet flow. The needles passed through the jet mixing region and the rule was completely outside the air flow, so the aerodynamic damping of the system was kept to a minimum. Figure 2 shows the anemometer wire set up in the jet, the pitot-tube and its manometer for measuring the jet speed, and the hot wire anemometer amplifier which was driven by the batteries in the base of the cart.

The motion of the wire (see Figure 3), was checked by means of a stroboscope and was determined to be simple harmonic, as would be expected. The beam was fairly stiff and the movement of the wire negligible until the beam was forced at its natural frequency. Movements up to 0.5 in. were easily attained at frequencies up to 250 cps. In order to get higher frequencies, a shorter beam would have to be utilized and the limiting case was nearly reached for the existing system. Several of the composite beams used suffered fatigue failures, and a very good bond between the rules was necessary if they were not to split apart after being vibrated for a short period. Several attempts were made to use the frequency associated with the second and higher modes of the beam to attain higher frequencies, but these were generally unsuccessful due to the bonding problems.

The natural frequency of the needles was much higher than the beam and they did not vibrate noticably, but the bond holding the needles to the rule failed several times at the highest frequencies. In order to extend this technique much above the frequency range used here, it will be necessary to construct special cantilever beams and holders for the wire to avoid the problems of beam and wire support failure.

A diagram of the complete apparatus used is shown in Figure 4. A typical experiment would involve positioning the wire in the core of the jet and constructing the static calibration for each wire. The wire was held still and the jet run at different speeds, whilst the mean dc voltage output of the hot wire anemometer was noted. The wire was then vibrated at various jet velocities within the calibration speed range. The electro-mechanical shaker was driven by a large amplifier controlled by an oscillator, and the frequency could be determined both from the oscillator and by viewing the output signal on a Cathode Ray Oscilloscope. The dc and rms voltage output of the anemometer amplifier were measured, and the signal was viewed on the CRO and recorded on tape for later analysis. The displacement of the wire was measured using the stroboscope, which allowed the wire motion to be viewed for regularity

over the full range of the wire movement. A final static calibration of the wire was then obtained, and compared to the initial result. If no significant differences were observed, the results were considered valid and analyzed.

The distance moved, and the frequency of oscillation of the wire, enabled the SHM velocity component of the wire movement to be calculated. This velocity was then added to the jet core velocity to obtain the complete description of the wire velocity. One complete velocity cycle was then used, with the static calibration curve, to construct one cycle of the voltage output that would be expected if the system was to operate exactly as for the static case. This result was then compared with the actual signal measured, the analysis for the latter case being carried over many cycles to obtain a mean result. The analysis of all the data was completed digitally. The values for the calculated voltage output were constructed from the appropriate equations for the motion and wire calibration and consisted of 100 voltages exactly covering one complete cycle. This data is referred to as Mathematical Data to distinguish it from the Experimental Data, which is the recorded output. The latter signals were played through the Analog-to-Digital Converters into the computer. Because of the low frequencies used, a sampling rate of 5200 samples per second was considered suitable. The data analysis was then completed on 2500 samples, which represents almost 0.5 sec. of data.

Certain parts of the experimental data showed irregularities, these being due to latent turbulence in the jet core and possible separation effects. These fluctuations will be discussed later, when the results are presented. In order to examine the full effects of these fluctuations, the digital results were smoothed by an additional computer program, and a second set of experimental results were obtained. To distinguish between the two sets of data, the original experimental values are referred to as "Experimental 1" in the figures and tables, and the smoothed results are indicated by "Experimental 2". The full analysis was completed on both sets of data.

Table 1 lists the measured quantities for each experiment. The principle inaccuracy will be in the determination of the displacement of the wire, which was only measured to an accuracy of 0.01 in. The voltages were read to three places, the frequency to 0.5 cps, and the air velocity to 0.01 in. on a vertical oil U-tube manometer. Four wires were used at four basic frequencies associated with the four beams used. A new wire was used for each beam because of the dangers of damaging the wire when the beam was modified.

TABLE I

VALUES MEASURED IN THE EXPERIMENTS

| Run No. | Wire No. | Voltage Output dc (volts) | Voltage Output rms | Air Velocity (fps) | Frequency (cps) | Displacement (in.) |
|---|---|---|---|---|---|---|
| 1 | 1 | 3.94 | 0.018 | 278 | 78.5 | - |
| 2 | 1 | 3.74 | 0.026 | 205 | 78.5 | 0.54 |
| 3 | 1 | 4.01 | 0.026 | 301 | 78.5 | 0.79 |
| 4 | 1 | 3.95 | 0.017 | 275 | 78.5 | 0.44 |
| 5 | 1 | 3.62 | 0.028 | 176 | 78.5 | 0.55 |
| 6 | 2 | 4.08 | 0.018 | 317 | 148.0 | 0.40 |
| 7 | 2 | 3.90 | 0.034 | 218 | 148.0 | 0.43 |
| 8 | 3 | 3.64 | 0.040 | 160 | 160.0 | 0.32 |
| 9 | 3 | 3.65 | 0.049 | 162 | 160.0 | 0.38 |
| 10 | 4 | 4.14 | 0.028 | 318 | 245.0 | 0.28 |
| 11 | 4 | 3.95 | 0.030 | 237 | 245.0 | 0.26 |
| 12 | 4 | 3.72 | 0.031 | 162 | 245.0 | 0.13 |
| 13 | 4 | 3.37 | 0.096 | 92 | 245.0 | 0.29 |
| 14 | 4 | 3.35 | 0.190 | 92 | 245.0 | 0.48 |
| 15 | 4 | 3.71 | 0.086 | 162 | 245.0 | 0.40 |
| 16 | 4 | 3.93 | 0.064 | 233 | 245.0 | 0.40 |

## 3.0 RESULTS AND ANALYSIS

### 3.1 Static Calibration of the Wires

The static calibration involved placing the wire in position in the core of the jet. A plot of the hot wire anemometer amplifier output voltage squared against the square root of the jet velocity produced the results shown in Figure 5. The calibration of volts against velocity is not linear, but the relationship plotted should be very near linear. The wire is heated by an electric current, and forms one arm of a bridge circuit. This bridge is kept in balance by a high gain amplifier, which adjusts the electric current to the wire to keep its resistance constant. The air flow cools the wire and draws more heat from the wire as the speed increases, so more current is necessary to maintain the bridge equilibrium. The constant temperature system is based on the wire being kept at a constant resistance, by a high gain feedback system, and hence, operates a nominally unvarying temperature, so that the thermal inertia of the wire is not critical when the system responds to rapid velocity fluctuations. As mentioned before, the fact that the temperature is not constant across the wire, and the temperature profiles change as the quantity of heat transfered varies, means that the thermal inertia will still be critical to some degree (Reference 10).

A relationship to describe the cooling of an electrically heated wire by an air flow was first derived by King (Reference 12), in terms of the electric heat input equaling the convected heat output. However, the heat transfer process is now normally expressed as a relationship between the normalized flow coefficients.

$$Nu = f(Re, Pr)$$

where $Nu$ is the Nusselt number $= \alpha d/k$

$Re$ is the Reynolds number $= \rho U d/\mu$

and $Pr$ is the Prandtl number $= C_p \mu/k$

$\alpha$ is the heat transfer coefficient

$d$ is the wire diameter

$k$ is the heat conductivity of the fluid

$\rho$ is the density of the fluid

$U$ is the air flow velocity

$\mu$ is the viscosity of the fluid

and $C_p$ is the specific heat of the fluid at constant pressure

An empirical expression derived by Kramers (Reference 13) has proved to be most representative of actual wire operation in subsonic incompressible flows.

$$Nu = A\, Pr^{0.2} + B\, Pr^{0.33}\, Re^{0.50} \qquad (1)$$

and typically $A = 0.42$ and $B = 0.57$

The voltage output of a constant temperature system is taken from across a bridge resistance or the bridge itself, and because of the constant resistance of the bridge, will be proportional to the current to the bridge, and the current through the wire. The heat input to the wire will be $I^2R$ where $I$ is the current through the wire and $R$ its resistance.

Therefore, the voltage output

$$E \sim I^{1/2} \sim \left(C + V^{1/2}\right)^{1/2}$$

and

$$E^2 = a\, V^{1/2} + b \qquad (2)$$

where $a$, $b$, and $C$ are empirical constants.

This result is based on an infinite wire length. The end effects, and varying temperature profile across the wire, cause small deviations from this relationship with real wires, and normally an experimental calibration is performed.

The results for the calibration achieved here are replotted in Figure 6 on a log basis in order to determine if a better expression to Equation (2) should be used in the calculations. A straight line is drawn through these plotted points, but the experimental scatter does not allow a better fit than was attained in Figure 5. Accordingly, Equation (2) will be used, and the values for the appropriate constants are given in Table II below.

TABLE II

STATIC CALIBRATION OF WIRES

| $E^2 = a\, V^{1/2} + b$ | | | | |
|---|---|---|---|---|
| Wire | a | b | $b^{1/2}$ | $E_o$ Volts |
| 1 | 0.757 | 3.04 | 1.741 | 1.67 |
| 2 | 0.741 | 4.31 | 2.075 | 1.73 |
| 3 | 0.663 | 4.90 | 2.21 | 1.81 |
| 4 | 0.723 | 4.33 | 2.08 | 1.70 |

This table also shows the voltage output of the amplifier measured at zero wind velocity, $E_o$. These values can be compared to the zero wind velocity values given by Equation (2); the square root of the constant b. The values given by the straight line fitted to the experimental results are higher, in all cases, than the measured voltage at zero velocity. It has further been shown (Reference 10) that this measured voltage is strictly too high, because, even when there is no applied air flow, the heat of the wire can cause substantial local convection. This means the extrapolated results are in a greater error than indicated by the results of Table II. This error is due to the equation not fully representing the behavior of the wire at very low velocities, when the end effects will be most important (Reference 10). However, the results measured here, and shown in Figure 5, suggest that within the range of air velocities used here, 80 to 312 fps, Equation (2) can be applied within the experimental scatter. Therefore, this expression was used to calculate the expected behavior of the wire based on the measured displacement of the wire in the dynamic calibration experiments.

The calculated output or Mathematical data, was based on the static calibration curve, and was obtained directly from the wire displacement and frequency, and the local speed of the jet core, as measured by the pitot-static tube.

$$U = -\frac{\omega d}{2} \sin(\omega t) + \bar{U} \qquad (3)$$

where d is the total displacement

$\bar{U}$ is the jet core velocity

$\omega$ is the radical frequency $= 2\pi f$

f is the frequency of oscillation.

and t is the time, whose origin is arbitrarily chosen to be when the wire is fully displaced.

This expression for the velocity was then used with Equation (2) to calculate the voltage output at 100 equal time intervals through one complete cycle. These basic 100 values were then used in the digital analysis programs to allow a direct comparison with the actual output voltages of the hot wire sets.

## 3.2 The Experimental Results

Figures 7, 8, 9, and 10 present typical results for the voltage output. The results for Run 7 are shown in Figure 7, where they are plotted automatically by the computer. It should be noted that different scales are used for the Mathematical and Experimental data, the actual scales being chosen to allow the results to be shown in the most effective manner. The Mathematical results are for the calculated output based on the wire static calibration and the measured displacement and frequency of the wire. Only one cycle is shown, since all the cycles are identical, and the analysis only involves one

complete cycle. However, a large number of cycles for the Experimental results had to be analysed to obtain a mean result, because of the small differences with this real signal. In these four figures, several cycles of the Experimental data are shown, and the differences can be observed.

Figure 8 shows one set of data for an early run. It was suspected that the air flow in the core of the jet was not perfectly laminar, and the results of this Figure shows the additional scatter to the basic fluctuating voltage. Several more screens were added in the settling chamber to eliminate this effect, after the results with Wire 1, Runs 1 to 5, were obtained.

Figures 9 and 10 show the results from two other runs, and also include a plot of the smoothed experimental results. The smoothing process causes a much more regular voltage output curve.

It was also noted, during the analysis of the results, that certain of the values for the rms voltage and the probability results showed irregularitites, and must be regarded as suspect data. It is believed the errors were due to incorrect settings of the tape recorder amplifiers. These suspect results are indicated in the tables, and are limited to Runs 1 and 15. All the results have been presented for completeness, but the values for these Runs have generally been ignored in calculating the mean differences between the Experimental and Mathematical data.

### 3.3 Rms Values

The data was first examined by comparing the rms values. Table III lists the intensities computed from the three sets of data. The first result is for the Mathematical data based on the results for the static calibration results, and the second and third values are for the experimental results of the actual oscillating wire output, as recorded and smoothed respectively.

The results were recorded on magnetic tape as an analog signal, while the rms level was noted during the recording on an rms voltmeter. The recording was then played through an amplifier to the Analog-to-Digital Converter and into the computer as a stream of digital data, and the rms values of these digital results was then computed. The various amplifiers were all set up on the results of certain runs; Run 1 for the wire Number 1, Run 8 for wires Number 2 and 3, and Run 12 for wire Number 4. The values given in Table IV show that the ratio of the directly measured rms value and the result calculated by the computer is near unity, for all except two runs. If the displacement of the wire is not measured exactly, then the rms voltage calculated from the static calibration will be inaccurate. The movement of the wire was noted by lining up a rule behind the wire, and as such will be inaccurate. The measurement was given to 0.01 in., but the accuracy is estimated to be no more than 3 percent.

TABLE III

RMS VOLTAGES OF THE DATA

| Run | Math | Rms Voltages Exp 1 | Exp 2 | $\frac{\text{Math}}{\text{Exp 1}}$ | $\frac{\text{Exp 1}}{\text{Exp 2}}$ | Wire |
|---|---|---|---|---|---|---|
| 1 | - | .01713 | .01660 | - | 1.032 | |
| 2 | .02775 | .02693 | .02657 | 1.030 | 1.014 | |
| 3 | .03053 | .02576 | .02544 | 1.185 | 1.013 | 1 |
| 4 | .01804 | .01665 | .01622 | 1.083 | 1.027 | |
| 5 | .03210 | .03090 | .03060 | 1.039 | 1.010 | |
| 6 | .02721 | .02623 | .02594 | 1.037 | 1.011 | 2 |
| 7 | .03568 | .03473 | .03441 | 1.027 | 1.010 | |
| 8 | .03410 | .03943 | .03902 | 0.865 | 1.011 | 3 |
| 9 | .04002 | .04951 | .04900 | 0.808 | 1.010 | |
| 10 | .03117 | .02940 | .02862 | 1.060 | 1.027 | |
| 11 | .03544 | .03864 | .03772 | 0.917 | 1.024 | |
| 12 | .02258 | .03111 | .03037 | 0.726 | 1.014 | |
| 13 | .07429 | .1023 | .09939 | 0.725 | 1.029 | 4 |
| 14 | .1243 | .1951 | .1896 | 0.637 | 1.029 | |
| 15 | .07275 | .09083 | .08686 | 0.801 | 1.046 | |
| 16 | .05491 | .06524 | .06373 | 0.842 | 1.024 | |

TABLE IV

RMS VOLTAGES OF EXPERIMENTAL RESULTS, BEFORE AND AFTER DATA ACQUISITION

| Run No. | Rms Measured (Volts) | Voltages From Data Reduction (Volts) | Measured Data |
|---|---|---|---|
| 1 | .018 | .01713 | 1.050 |
| 2 | .026 | .02693 | .966 |
| 3 | .026 | .02576 | 1.010 |
| 4 | .017 | .01665 | 1.021 |
| 5 | .028 | .03090 | .907 |
| 6 | .018 | .02623 | .686 |
| 7 | .034 | .03473 | .980 |
| 8 | .040 | .03943 | 1.014 |
| 9 | .049 | .04951 | .989 |
| 10 | .028 | .02940 | .953 |
| 11 | .030 | .03864 | .776 |
| 12 | .031 | .03111 | .996 |
| 13 | .096 | .1023 | .938 |
| 14 | .190 | .1951 | .974 |
| 15 | .086 | .09083 | .946 |
| 16 | .064 | .06524 | .982 |

Because the rms voltages are not exactly the same, an exact comparison of the results is not possible, and they cannot be compared directly to look for small differences. However, if the basic mechanism of the convective heat transfer process is changed in the dynamic case, then the "shape" of the resultant voltage fluctuations could be expected to be different.

## 3.4 The Probability Function

The curves of the voltage output were first examined on a probability density basis. In fact the computer calculated the Probability Function for each of the three sets of data for each run (see Appendices A and B).

Figure 11 shows the measured Probability Function $F(\zeta)$ for the results of Run 2, where $\zeta$ is the normalized voltage, and equals 0 for the minimum voltage of the sample and 1.0 for the maximum value. The results for a sine wave are included, as are the calculated values for the Mathematical data and the two sets of Experimental data. The results fall into two sets. The Mathematical data, for the calculated response based on the static calibration curve, agrees very well with the sine wave result. The slight difference is because the static calibration is not linear, but is nearly so over the velocity range of the experiment. The two experimental results show a different shape, and this is directly due to irregularities in the experimental signal. Within each sample there are apparently a few peaks with a higher voltage, both positive and negative, and this causes the change in the Probability Function curves at the extremes of voltage. Figure 12 shows a similar set of results for Run 8, although the effect is not quite so pronounced here. For the sample chosen for Run 15, where Probability Function is plotted in Figure 13, a very large negative peak has apparently been included, so the results show the highly unbalanced Probability function Curves for the Experimental data.

In Figures 14 and 15, the Probability Functions are plotted against actual voltage rather than a normalized value. The experimentally measured result, the calculated Mathematical values based on the static calibration, and the Mathematical values multiplied by the ratio of the rms voltages are shown. These results show good agreement for both the results of Run 8 and the data of Run 15. In the latter case the highly unbalanced Probability Function curve is shown in its correct perspective with a very negative peak voltage apparently included. The data for the corrected Mathematical example shows the best agreement, and suggests that the difference in the curves is limited to the extreme values of the Probability Function, and the difference between the values of the first set of Mathematical data and the Experimental results is purely due to errors in the calibration of the various amplifiers of the tape recorder and in line to the Analog-to-Digital Converter.

The results show that the major difference between the Experimental and Mathematical results is limited to the extreme values of voltage. The analysis shows that the Experimental data results have higher peak values than the results for the sine wave voltage output of the Mathematical data. Apparently, the Experimental output voltage contains excursions of 20% beyond the expected peak levels, and this must change the shape of the output voltage curves. The peaks will be much sharper than for the smooth calculated sine wave values, and the exact extent of this difference will be examined in the next subsection.

## 3.5 Curve Analysis

The differences between the measured output voltages and the calculated values, determined from the static calibration, were examined by a probability factor analysis of the signals. Appendices A and B give the definition of the factors and details of the computer technique used to calculate the actual values. The results calculated for the Form, Skewness, and Flatness Factors are listed in Table V for the three sets of data for each Run. The mean values, and ratios between the results for the different sets of data and the values for a sine wave, are also presented.

The results for the Form Factor for the dynamic calibration voltage signal, all show a higher value than for the voltage calculated directly from the static calibration. The latter results are in agreement with the sine wave value, except for Run 14, when the maximum displacement occurred. For the smoothed experimental results, the mean value of the Form Factor was 1 percent greater than the calculated result. The difference is due to the higher peak voltages obtained in the dynamic calibration case.

The results for the Skewness Factor, for the Mathematical data, are all just negative. This is expected, since the response of hot wire anemometers is not linear. At the lower velocities, the voltage response for a given velocity increase will be greater. Therefore, when a regular curve of velocity, such as Simple Harmonic Motion of the wire, is used to calculate the voltage output from this system, the negative peaks of voltage of the ac part of the signal will be slightly higher and more sharply peaked. The effect is small since the variation over the range of velocity used is small. The greatest effect should be noticed at the lower velocities, that is Runs 5, 8, 9, 13, and 14, and these results do show the greatest skewness. The value for Run 14 is the largest, and could be in error. The mean value for the Skewness Factor calculates as -0.03577 including Run 14, and -0.02775 ignoring this run. The results for the Experimental data shows a wide scatter, with both negative and positive values. For these Experimental results, the Skewness Factor of Run 14 is again large, but the greatest value was found for Run 1. Because of the wide scatter of the results, and because they are all near zero, the ratio of the Skewness Factor values for the Mathematical data has little meaning. Therefore, they will not be examined any further, and no mean values are presented.

For the Flatness Factor results, the mean value for the Mathematical data is 1.503, just greater than the value for a sine wave at 1.500. This small difference is due to the non-linear operation of the wire, and shows the slightly more peaked negative part of the voltage output signal. The values for the Experimental data show significant increases in the Flatness Factor from the sine wave value. The mean value of the 14 results, the two largest results of Runs 1 and 15 are ignored as being in error, is 1.588, an increase of 6 percent. For the smoothed experimental results, the mean value of this factor becomes 1.567. The greatest difference from the sine wave results occurs for those runs with the largest velocity variation, Runs 13, 14, and 15, as before. The results for Runs 4 and 5 also show a significant difference. In Table V, the ratios of

TABLE V

CURVE ANALYSIS

| Run | Wire | Form Factor | | | Skewness Factor | | | Flatness Factor | | |
|---|---|---|---|---|---|---|---|---|---|---|
| | | Math | Exp 1 | Exp 2 | Math | Exp 1 | Exp 2 | Math | Exp 1 | Exp 2 |
| 1 | | - | 1.319 | 1.283 | - | (0.1589) | (0.2164) | - | (2.013) | (1.724) |
| 2 | | 1.234 | 1.263 | 1.252 | -0.01982 | -0.02356 | -0.01820 | 1.501 | 1.642 | 1.588 |
| 3 | 1 | 1.234 | 1.255 | 1.246 | -0.01962 | -0.01793 | -0.01327 | 1.501 | 1.605 | 1.561 |
| 4 | | 1.234 | 1.307 | 1.277 | -0.01186 | -0.00670 | -0.01313 | 1.500 | 1.784 | 1.660 |
| 5 | | 1.234 | 1.263 | 1.253 | -0.02424 | -0.06778 | -0.06050 | 1.501 | 1.625 | 1.588 |
| 6 | 2 | 1.234 | 1.251 | 1.247 | -0.01781 | 0.00141 | 0.00626 | 1.500 | 1.595 | 1.578 |
| 7 | | 1.234 | 1.231 | 1.231 | -0.02534 | 0.01919 | 0.02034 | 1.501 | 1.511 | 1.506 |
| 8 | 3 | 1.234 | 1.240 | 1.240 | -0.02930 | 0.03616 | 0.03549 | 1.501 | 1.537 | 1.532 |
| 9 | | 1.234 | 1.240 | 1.238 | -0.03418 | 0.03257 | 0.03093 | 1.502 | 1.517 | 1.513 |
| 10 | | 1.234 | 1.244 | 1.242 | -0.02072 | 0.02536 | 0.02685 | 1.501 | 1.551 | 1.535 |
| 11 | | 1.234 | 1.240 | 1.238 | -0.02562 | 0.01401 | 0.01475 | 1.501 | 1.522 | 1.519 |
| 12 | | 1.234 | 1.245 | 1.245 | -0.01809 | 0.01135 | 0.00977 | 1.500 | 1.552 | 1.548 |
| 13 | 4 | 1.234 | 1.255 | 1.245 | -0.07088 | 0.00523 | 0.01385 | 1.507 | 1.631 | 1.565 |
| 14 | | 1.238 | 1.248 | 1.240 | -0.1197 | 0.1541 | 0.1735 | 1.520 | 1.641 | 1.544 |
| 15 | | 1.234 | 1.278 | 1.245 | -0.05952 | -0.1188 | 0.03570 | 1.505 | (2.903) | 1.597 |
| 16 | | 1.234 | 1.235 | 1.235 | -0.03981 | 0.5818 | 0.05470 | 1.502 | 1.514 | 1.512 |
| Mean | | 1.234 | 1.257 | 1.247 | -0.03577 | | | 1.503 | 1.696 | 1.567 |
| | | | | | | | | | 1.588 | |
| Sine Wave | | 1.234 | | | 0.0 | | | | 1.500 | |

The circles around particular values indicate suspect numbers. The mean values are calculated both including and excluding these values for the Flatness Factor, Exp 1 results.

TABLE V

CURVE ANALYSIS
(Concluded)

| Run | Wire | Form Factor Ratio | | Skewness Factor Ratio | | Flatness Factor Ratio | |
|---|---|---|---|---|---|---|---|
| | | Exp 1 / Math | Exp 2 / Math | Exp 1 / Math | Exp 2 / Math | Exp 1 / Math | Exp 2 / Math |
| 2 | 1 | 1.024 | 1.015 | 1.189 | 0.918 | 1.094 | 1.058 |
| 3 | | 1.017 | 1.010 | 0.914 | 0.676 | 1.069 | 1.040 |
| 4 | | 1.059 | 1.035 | 0.565 | 1.107 | 1.189 | 1.107 |
| 5 | | 1.024 | 1.015 | 2.796 | 2.496 | 1.083 | 1.058 |
| 6 | 2 | 1.014 | 1.011 | -0.079 | -0.364 | 1.063 | 1.052 |
| 7 | | 0.998 | 0.998 | -0.753 | -0.803 | 1.007 | 1.003 |
| 8 | 3 | 1.005 | 1.005 | -1.224 | -1.211 | 1.024 | 1.021 |
| 9 | | 1.005 | 1.003 | -0.953 | -0.905 | 1.010 | 1.007 |
| 10 | 4 | 1.008 | 1.006 | -1.224 | -1.296 | 1.033 | 1.023 |
| 11 | | 1.005 | 1.002 | -0.547 | -0.576 | 1.014 | 1.012 |
| 12 | | 1.009 | 1.009 | -0.627 | -0.540 | 1.035 | 1.032 |
| 13 | | 1.017 | 1.009 | -0.074 | -0.195 | 1.082 | 1.038 |
| 14 | | 1.008 | 1.002 | -1.294 | -1.431 | 1.080 | 1.016 |
| 15 | | 1.036 | 1.009 | 1.996 | -0.600 | (1.929) | 1.061 |
| 16 | | 1.001 | 1.001 | -1.485 | -1.148 | 1.008 | 1.007 |
| Mean | | 1.015 | 1.009 | | | 1.052<br>(1.115) | 1.036 |

the results for the Experimental and Mathematical data show that the mean increase for the measured voltage outputs is 5 percent over the calculated values. For the smoothed Experimental voltages, the increase is near 4 percent. This difference, and especially the difference noted for the results with the largest fluctuating velocity components, show that the voltage output curves will be significantly more peaked than the expected calculated results.

These results will be discussed in the next section.

## 4.0 DISCUSSION

The objective of the experiment was to develop a technique for the dynamic calibration of hot wire anemometers. The method used here is initially limited to low frequencies by the mechanical restrictions of the system, and so will not be useful for examining thermal inertia effects of the wire and the surrounding air stream. However, the system will still prove useful as allowing an accurate dynamic calibration, and further some small effects were noticed. These are considered as being due to the aerodynamic inertia of the flow over the wire, and the resulting changes in the viscous convective cooling process. All previous work, to study the dynamic behavior of hot wire anemometers, has been based on either calculations or measurements on the system when voltage transients are applied to the apparatus, and it is assumed that the wire-air cooling process reacts sufficiently quickly that it can be neglected.

The intensity of the velocity fluctuations, as well as the frequency of the turbulence measured, will also be important in studying the dynamic behavior of the system. The intensity of the velocity fluctuations produced in the experiments was generally low, with the highest velocity variation being obtained during Run 14. Here the maximum velocity component was calculated as ± 30 fps, giving a velocity variation from 61 to 123 fps, which for a sine wave gives an intensity, normalized on the mean velocity, of 16.7 percent. At these lower frequencies of wire movement, the velocity variations were not so great. For example, in Run 5, the velocity fluctuations peaked at ±11.3 fps, to give a velocity range from 165 to 187fps, and a corresponding intensity of 3.2 percent. The full list of intensities is included in Table VI. Any effects would be expected to show up most for those runs where the greatest fluctuating velocity compartment was applied, and therefore, the results of Runs 13, 14, and 15 will be particularly considered.

The Reynolds number range of the wire in these examples is from approximately 7 to 39, based on the mean velocities plus the highest fluctuating velocity component. The flow pattern of a steady incompressible flow around a cylinder exhibits changes at Reynolds numbers of 10 and 40, and possible effects due to this variation could occur. It is generally considered that the basic cooling equilibrium expression of Equation (1) applies throughout the normal operating range of a small diameter hot wire anemometer, but that different values of the constants may occur in each Reynolds number range. Therefore, it will be concluded that the flow over the wires should be similar for the whole range of velocities considered here. No variation due to a basic change in the flow pattern can be expected, and all differences must be due to the fluctuating nature of the flow.

The differences between the output voltages of the measured signals and the calculated values were examined by determining the statistical probability factors of the voltage output curves. Although this technique is more normally applied to random signal analysis, the results can be applied to the regular voltage output signals obtained here.

TABLE VI

INTENSITY OF THE APPLIED VELOCITY FLUCTUATIONS

| Run | Wire | Maximum Fluctuating Velocity Component $u_{max}$ (fps) | Mean Velocity (fps) | Intensity of Velocity Fluctuations $\frac{\left(\overline{u^2}\right)^{1/2}}{V}$ |
|---|---|---|---|---|
| 1 | | - | 278 | - |
| 2 | | 11.1 | 205 | 0.027 |
| 3 | 1 | 16.2 | 301 | 0.027 |
| 4 | | 9.1 | 275 | 0.017 |
| 5 | | 11.3 | 176 | 0.032 |
| 6 | 2 | 15.3 | 311 | 0.025 |
| 7 | | 16.7 | 218 | 0.038 |
| 8 | 3 | 13.6 | 160 | 0.043 |
| 9 | | 16.1 | 162 | 0.050 |
| 10 | | 17.7 | 318 | 0.028 |
| 11 | | 16.9 | 337 | 0.036 |
| 12 | | 8.5 | 162 | 0.026 |
| 13 | 4 | 18.5 | 92 | 0.101 |
| 14 | | 30.8 | 92 | 0.167 |
| 15 | | 25.4 | 162 | 0.078 |
| 16 | | 25.4 | 233 | 0.055 |

The values for the Form Factor only show a small effect, but do indicate the larger values obtained with the dynamic calibration technique. The results for the Skewness Factor do not indicate any significant result because of the scatter. The numbers are based on the difference between two summations of the negative and positive parts, and so a small effect can cause a large change in the resultant value. Even so, the largest values of Skewness Factor occur for Runs 13 and 14, which have the largest intensity values of the applied velocity fluctuations. There is also one additional point that must be mentioned here concerning these results, since it will tend to eliminate some of the differences between the two sets of voltage output. In the calculation of the Mathematical data, the velocity fluctuations are evenly applied about a given mean value, and the mean of the fluctuating velocity component is zero. However, when the voltage output is calculated from the static calibration curve, the mean of the fluctuating voltage component formed will not be exactly zero, because of the non-linear nature of the wire operation. For the experimental results, the voltage output is automatically given a mean value of zero, because of the ac amplifiers used in the circuit. Therefore, the origin for the experimental voltage fluctuations will be shifted slightly from the voltage corresponding to the mean velocity. This effect will tend to depreciate the difference in the negative and positive part of the fluctuating voltage signal, and give a more even result for the curve factors used here. Hence, the true differences between the results for the Mathematical and Experimental data will be greater. This does not explain why the Skewness Factor is negative for all the results of Wire 1 and for Run 15, while positive for all the other experimental cases. It could be due to incorrect setting up of the amplifiers for the Analog-to-Digital Converters which would explain the Skewness Factor results for Run 1 to 5, but not the sign change noted in Run 15.

The results for the Flatness Factor are most significant. They always show higher values for the Experimental data, compared to the results for the Mathematical data and a sine wave. Runs 13, 14, and 15, where the high fluctuating velocity intensities occur, all give high values of the Flatness Factor. The results for Wire 1, Runs 1 to 5, also show high values of the Flatness Factor, but these were obtained in a more turbulent flow, and these high values are assumed to be a direct consequence of this increased turbulence. If the results of Wire 1 are ignored, then the remaining results show a trend of increasing Flatness Factor with increasing intensity of the velocity fluctuations. There is a considerable variation in the results, with Run 6 giving a high Flatness Factor for a low fluctuating velocity intensity, and Run 16 producing a smaller value of Flatness Factor with a greater intensity. However, there is a general trend, and it indicates that the output voltage curves for the experiments are more peaked than for the calculated output from the static calibrations. This result confirms the indications of the Form Factor results.

The analysis of the turbulence in the center of a subsonic jet mixing region, using hot wire anemometers, has shown that the statistical distribution of the components of the velocity fluctuations is Gaussian, (Reference 15). Since turbulence is a completely random motion, this is a perfectly logical result, and the accuracy with which the hot wire signals produce this result does tend to suggest that they are measuring the velocity components exactly. However, the results obtained here could still indicate that there are effects due to the changing air flow over the wire, which means the static convection cooling laws are not immediately duplicated in the dynamic case. For example, the results of Run 14 suggest this could be happening when a large velocity fluctuation occurs at a small mean velocity. Another possible example is the operation of the wires in a rarefied gas, when the Reynolds number of the flow will be very small. These results therefore indicate the advantages of a dynamic calibration technique.

A final point concerns the use of hot wire anemometers in supersonic flows. Here the formation of a shock wave by the probe and wire makes the operation of the system more complicated. A fluctuating velocity in the flow means that the shock wave pattern will change and this could cause the flow pattern over the wire to change and alter the cooling process. It is obvious that the calibration technique should be extended to examine the effects in supersonic flow, although, because of the increase in air velocity, it may prove difficult to obtain high intensities of the velocity fluctuations.

With different materials and better constructed beams, it should prove possible to increase the frequency range of the dynamic calibration system to near 1000 cps. This is not really high enough, and other problems, such as the aerodynamic damping and the mass inertia of the wire and its supports, could become critical. The motion of the wire would have to be more carefully examined, and a photographic technique will probably be necessary. However, it would probably be worthwhile to continue these experiments, especially for the supersonic flow case.

## 5.0 CONCLUSIONS

A technique for dynamically calibrating hot wires has been presented. This method is based on moving the wire with known Simple Harmonic Motion, by using an oscillating cantilever beam, in a steady air stream. The air velocity applied to the wire can then be calculated from the measured wire displacement and frequency, and the absolute dynamic calibration obtained.

The present system is limited to low frequencies, and so thermal interia effects of the system will be negligible. Therefore, any effects measured were considered the result of the aerodynamic convective cooling process, and indicate a change from the normally assumed static calibration conditions.

The output from the constant temperature hot wire anemometer was compared to a calculated signal, determined from the static calibration of the hot wire system and the motion of the wire. The measured signal was found to give close agreement with the calculated signal. However, the experimental output voltage signal was noted to have generally larger values of both the Form Factor and the Flatness Factor, compared to the calculated output based on the static calibration curve. This indicates that a more peaked signal is created here, and it is concluded that some small deviation is occuring from the steady flow case due to the convective cooling changing with the rapidly changing airflow. This will not be concerned with the thermal inertia of the air surrounding the wire, because of the small size of the wire and the low frequency oscillations, but must be due to a change in the cooling process as the velocity over the wire changes.

For measurements limited to the frequency range considered here, the static calibration technique will be more useful, since it is considerably simpler, and the error will be small. However, for use in very low mean velocities, with large fluctuating velocity components, it may prove incorrect and a more fundamental dynamic calibration method would be necessary. It could be especially relevant when the very turbulent shear flow of jets and rocket exhaust flows are examined. The dynamic calibration technique could also be useful when measurements are to be made in a rarefied gas, or at supersonic speeds. For the latter case, the movement of the shock pattern around the wire and probe could become important, and a much different convective cooling process formed.

It is therefore recommended that these studies continue, directed at increasing the frequency of the oscillation of the beam. If higher frequencies can be attained then the velocity of the jet should be increased to supersonic speed.

## APPENDIX A

## PROBABILITY ANALYSIS OF THE RESULTS

The Probability Density $p(x)$ is defined as the probability that a signal exists between the limits $x$ and $(x + \delta x)$ at any given time. However, for experimental reasons, it is often easier to measure the time a signal exceeds a given reference value of $x$ in a given period, and this is defined as the Probability Function, where

$$F(x) = \int_{x}^{+\infty} p(x)\, dx \qquad (A.1)$$

The Probability Density is usually normalized, so that

$$\int_{-\infty}^{+\infty} p(x)\, dx = 1.0 \qquad (A.2)$$

Then $F(-\infty) = 1.0$

$F(+\infty) = 0$

The Probability Density is the derivative of the Probability Function, and experimental values are obtained by measuring the slope of the Probability Function curve.

$$p(x) = - dF(x)/ dx \qquad (A.3)$$

For a real sample of data, a maximum and a minimum voltage will occur. Say they are $x_{max}$ and $x_{min}$. Then

$$F(x_{min}) = 1.0$$

$$F(x_{max}) = 0$$

and the values of the Probability Function are 1.0 for all values of $x$ below $x_{min}$, and 0 for all values of $x$ above $x_{max}$, since no signal occurs here in the sample.

The Probability Density curve helps to describe the shape of random and regular signals, and the Probability Function curve can be interpreted this way also. The mathematical moments of the probability density curve give a quantitative description of the signal. The moments are defined as ,

$$\overline{V^n} = \int_{-\infty}^{\infty} x^n p(x)\, dx \qquad (A.4)$$

where $x = 0$ is the mean value about which these moments are taken. For the first moment the absolute value of $x$ is used to obtain a value other than zero. The following factors can then be defined,

Form Factor $\quad C = \overline{V^2} \Big/ |\overline{V}|^2$

Skewness Factor $\quad S = \overline{V^3} \Big/ \left(\overline{V^2}\right)^{3/2}$

Flatness Factor $\quad F = \overline{V^4} \Big/ \left(\overline{V^2}\right)^2$

These moments can be calculated either from the Probability Density values, or from the Probability Function values, as described in Reference 15. However, in this experiment, where the data was digitized, the effective Probability Density was measured, and the moments were calculated directly from the digital values.

The three factors defined above can be used to examine both regular and random signals, and also to describe the "shape" of the signals. The Form Factor is a normalized rms result, relating the square to the mean of the voltage. The Skewness Factor directly compares the negative and positive parts of the signal. A regular curve with exactly equal absolute values for the two parts will have a Skewness Factor of zero, as will a random signal with a perfectly symmetrical Probability Density distribution. The Flatness Factor is weighted towards the larger absolute values of the data, because of the values raised to the fourth power. This factor describes the amount of signal farthest away from the zero mean value. A very sharply peaked curve will have a larger Flatness Factor, and a very broadly peaked curve will have smaller values of this factor. The difference occurs, because the factor is normalized on the rms value.

Table A-I lists the values of these factors for three typical examples. First, a random signal where the distribution is Gaussian, secondly, for a square wave signal, and finally, for a sine wave signal. The latter case is of interest here, since the velocity fluctuation of the applied flow to the wire will be a sine wave.

TABLE A-I

PROBABILITY FACTORS FOR VARIOUS SIGNALS

| Signal | Form Factor C | Skewness Factor S | Flatness Factor F |
|---|---|---|---|
| Random Gaussian | $\pi/2$ | 0 | 3.000 |
| Square Wave | 1.000 | 0 | 1.000 |
| Sine Wave | $\pi^2/8 = 1.234$ | 0 | 1.500 |

## APPENDIX B

## COMPUTER PROGRAM USED IN ANALYSIS

Figure 16 is a flow diagram of the analysis program for the data. Basically the program calculated 100 values of Mathematical data covering exactly one cycle, based on the static calibration. Since all cycles of this Mathematical data are equal, only one complete cycle is needed here. For the Experimental data, a sample of 2500 values was taken for each run. These results were recorded at 5200 digital values per second, which represents nearly 0.5 seconds of sample. This may not be sufficiently long enough for the lowest frequencies, but the consistency of the answers suggests that is probably satisfactory. Errors of up to 2 percent may be possible at these lower frequencies.

The smoothed Experimental data, Experiment 2, was generated by including a smoothing program in the main program, and this subroutine and the plotting routines could be selected as required by switches.

The Probability Function was determined by directly counting the number of digital data values that exceeded the reference levels. These reference levels were chosen such that the negative and positive range of the data were each covered in 12 equal steps.

The moments for the Probability analysis were calculated directly from the digital values. Each value was raised to the appropriate power, the answers added, and finally normalized by dividing by the total number of samples.

## REFERENCES


1. Hinze, J. O., "Turbulence", Chap. 2, McGraw-Hill Book Co., Inc., 1959

2. Kovasznay, L. S. G., "The Hot Wire Anemometer", Acta Tech., Acad. Sci. Hungaricae, Budepest, Vol. 50, 1965

3. Wise, B., et al., "The Hot-Wire Anemometer for Turbulence Measurements", Parts 1, 2, 3, and 4, British ARC Reports 13,803, 14,285, 16,679 and 16,726, 1951 - 1954

4. Bradshaw, P. and Johnson, R. F., "Turbulence Measurements with Hot Wire Anemometers", British N.P.L., Notes on Applied Sciences No. 33, HMSO London, 1963

5. Kovasznay, L. S. G., "Development of Turbulence-Measuring Equipment", NACA Report 1209, 1954

6. Laurence J. C. and Landes, L. G., "Auxiliary Equipment and Techniques for Adapting the Constant-Temperature Hot-Wire Anemometer to Specific Problems in Air-Flow Measurements", NACA Technical Note 2843, 1952

7. Morkovin, M. V. and Phinney, R. E., "Extended Applications of Hot-Wire Anemometry to High-Speed Turbulent Boundary Layers", AFOSR TN-58-469, 1958

8. Demetriades, A., "Hot-Wire Measurements in the Hypersonic Wake of a Cylinder", Jour. Aero. Sci., Vol. 28, No. 11, 1961

9. Potter, R. C., "The Hot Wire Anemometer", Wyle Laboratories Research Staff, Report WR 64-8, 1964

10. Davies, P. O. A. L. and Fisher, M. J., "Heat Transfer from Electrically Heated Cylinders", Proc. Roy. Soc. A, Vol. 280, 1964

11. Corrsin, S., "Directional Sensitivity for a Finite Hot-Wire Anemometer", AFOSR TN-60-171, 1960

12. King, L. V., "On the Convection of Heat from Small Cylinders in a Stream of Fluid", Phil. Trans. Roy. Soc. A, Vol. 214, 1914

13. Kramers, H., "Heat Transfer from Spheres to Flowing Media", Physica Vol. 12, 1946

14. Corrsin, S., "Turbulence: Experimental Methods", Encyclopedia of Physics, Vol. VIII/2, pp. 521 - 590, Springer-Verlag, Berlin, 1963

15. Davies, P. O. A. L. and Fisher, M. J., "Statistical Properties of the Turbulent Velocity Fluctuations in the Mixing Region of a Round Subsonic Jet", Univeristy of Southampton, England, AASU Rep. 233, 1963

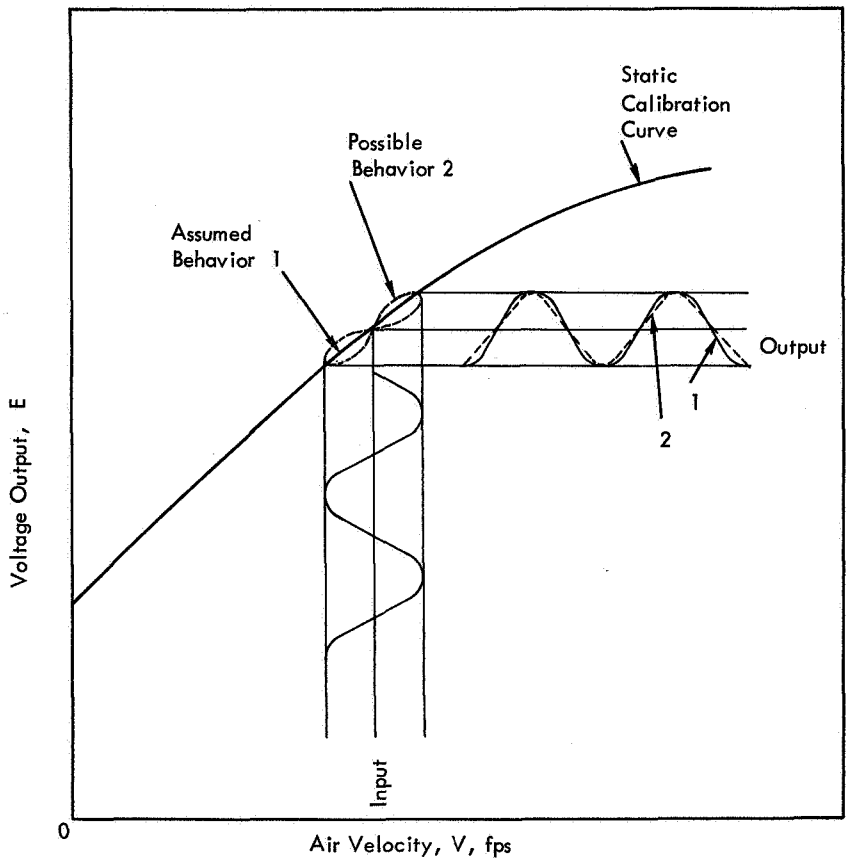


Figure 1. Hot Wire Anemometer Operation Characteristics

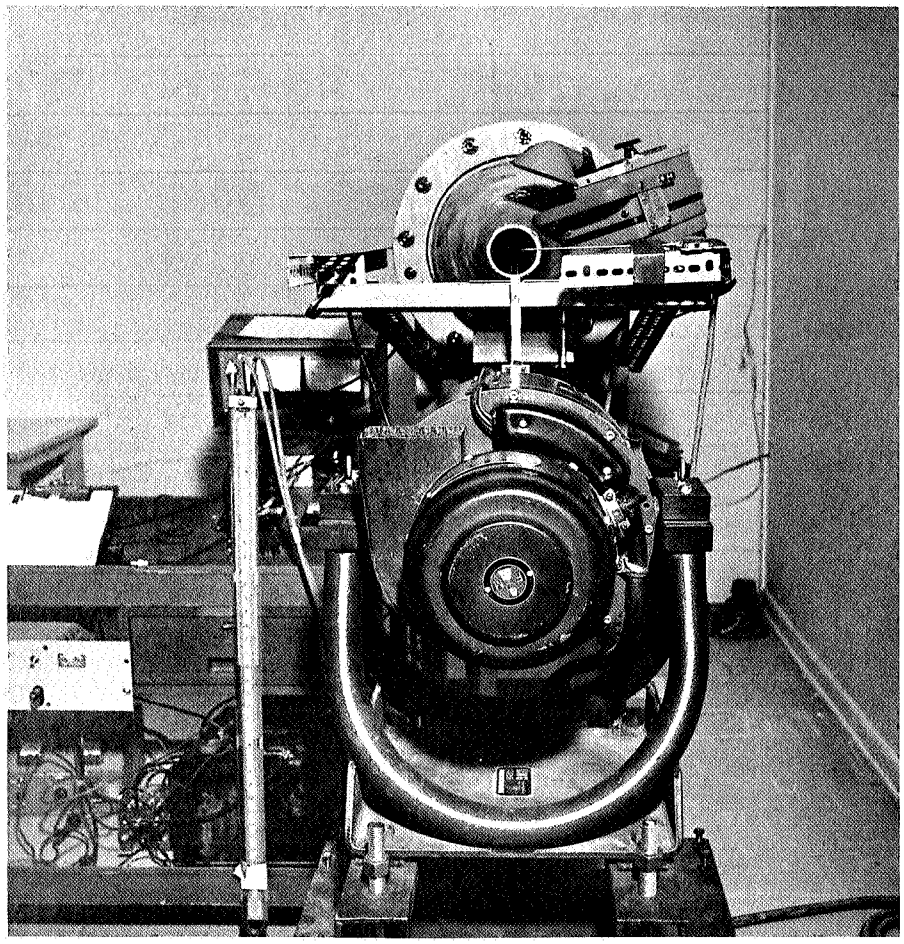

Figure 2. View of Experimental Rig

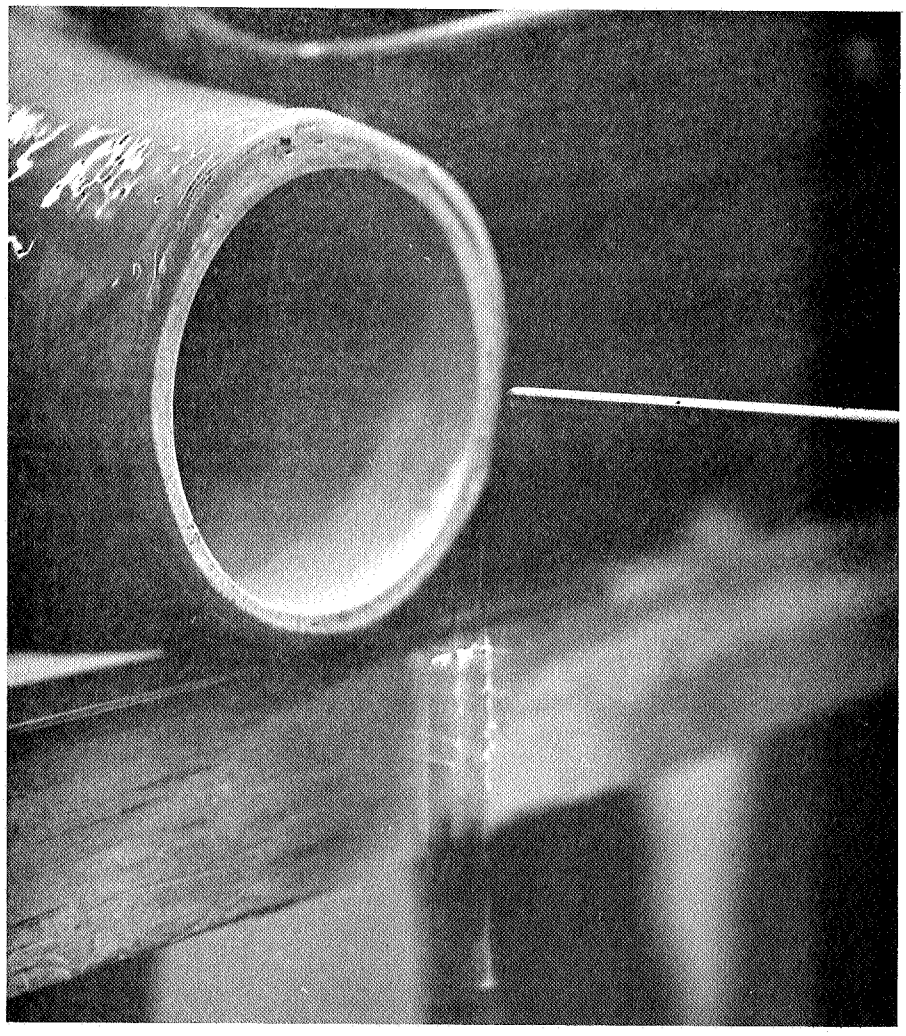

Figure 3. Wire Vibrating in Core of Jet

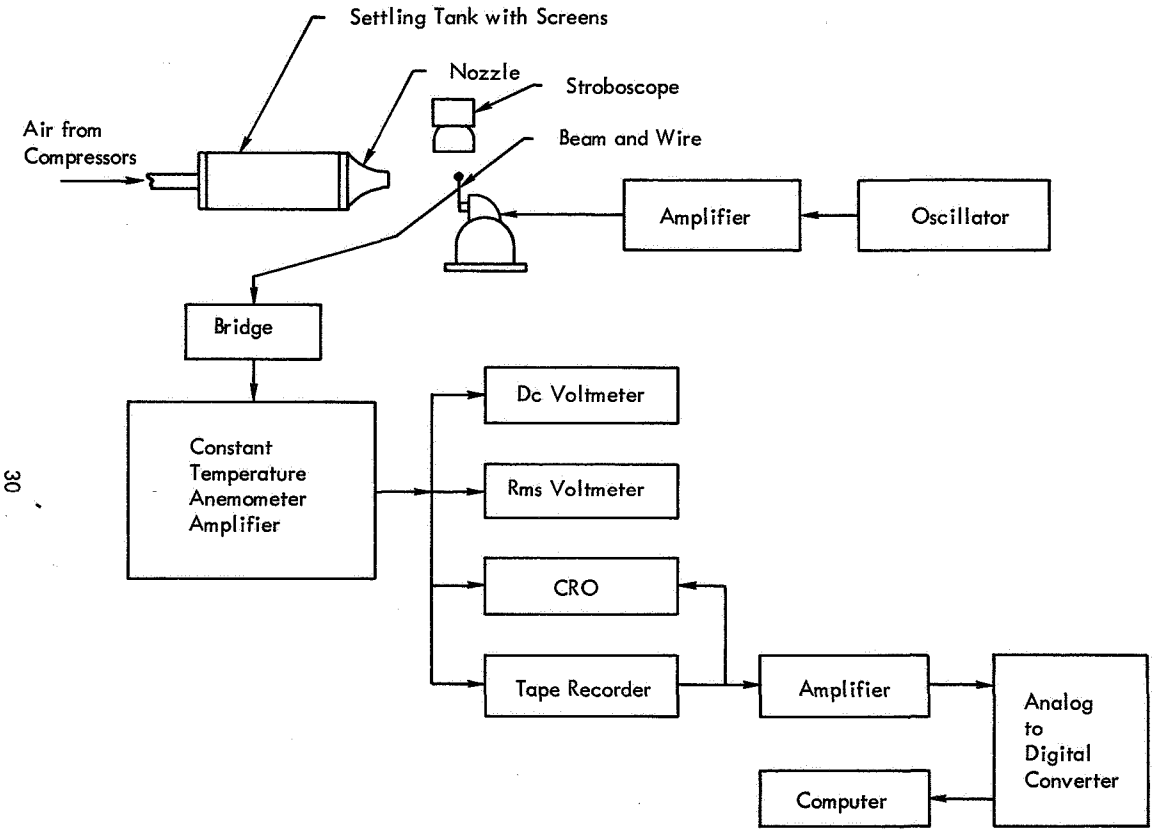


Figure 4. Diagram of Apparatus

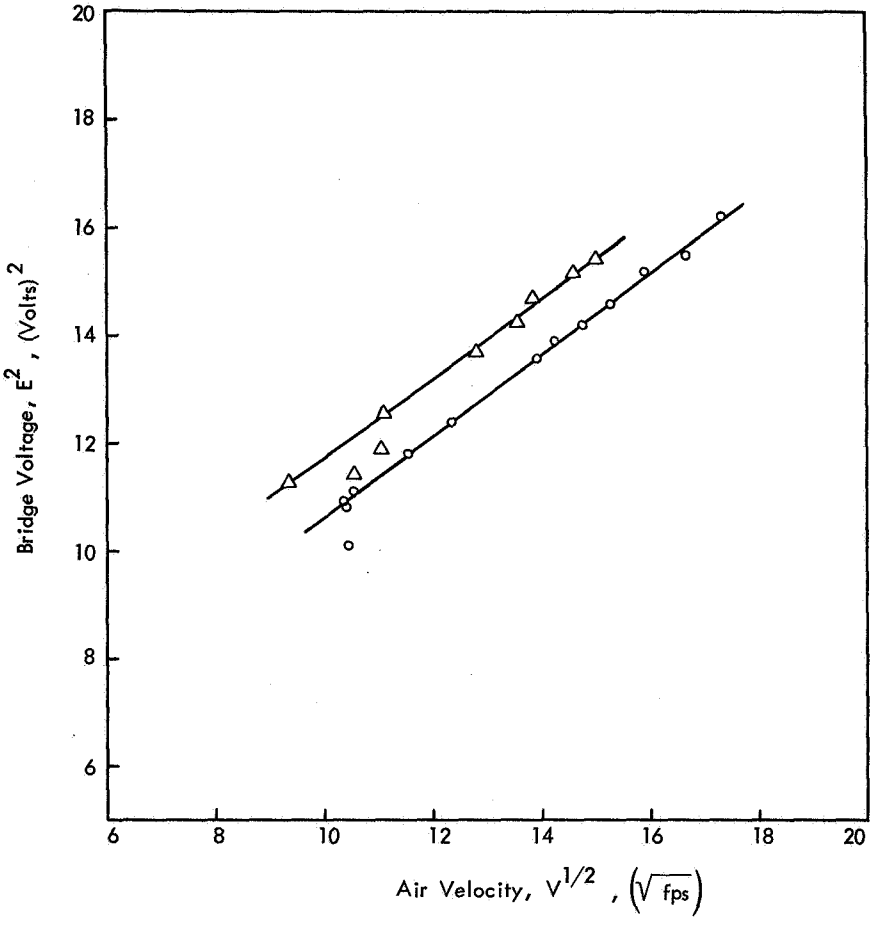


o Wire 1
△ Wire 2

Figure 5a. Static Calibration of Wires

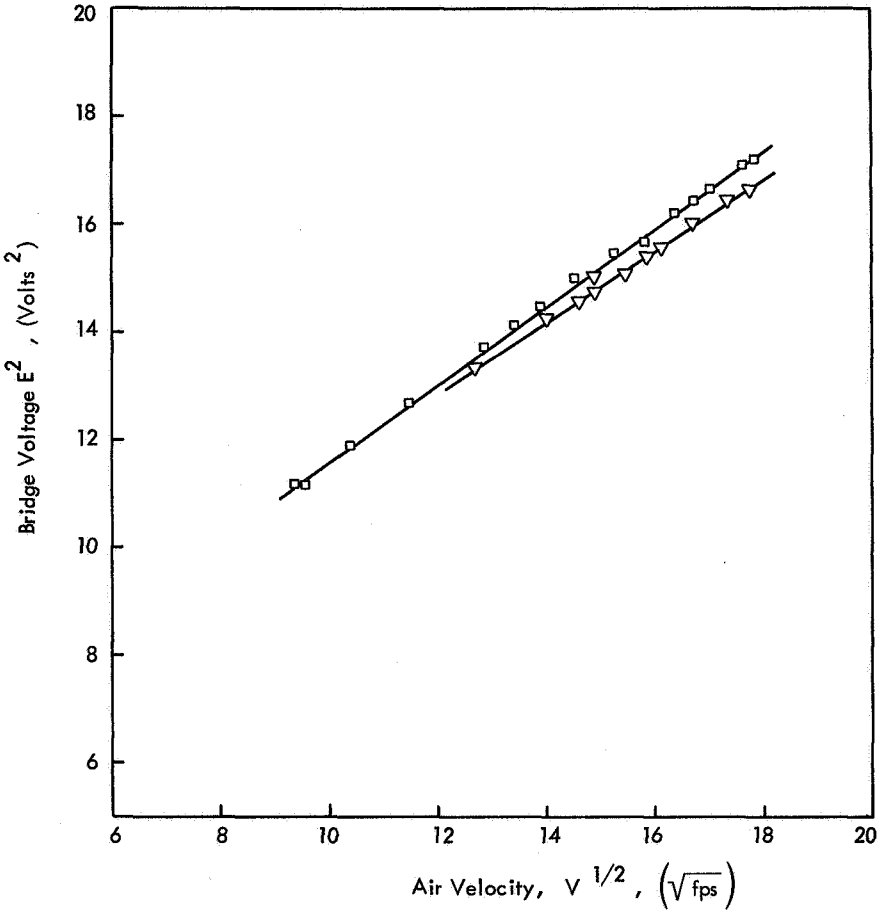


Figure 5b. Static Calibration of Wires (Concluded)

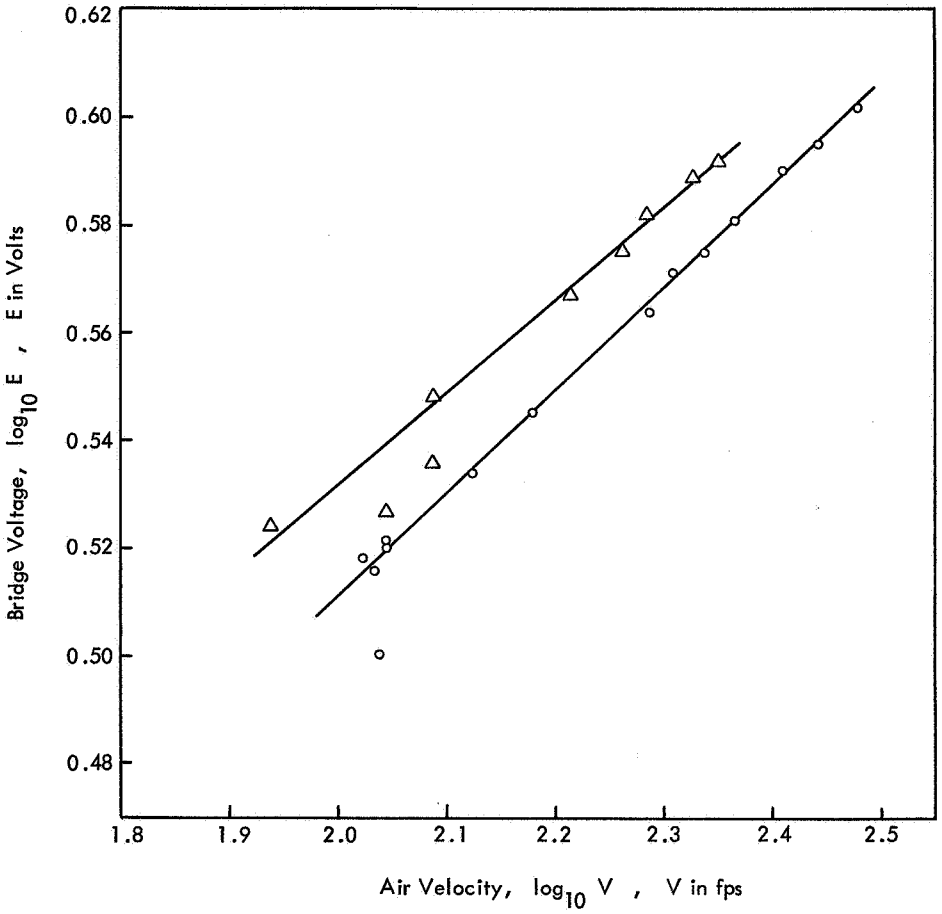


o Wire 1

Δ Wire 2

Figure 6a. Static Calibration of Wires, (log basis)

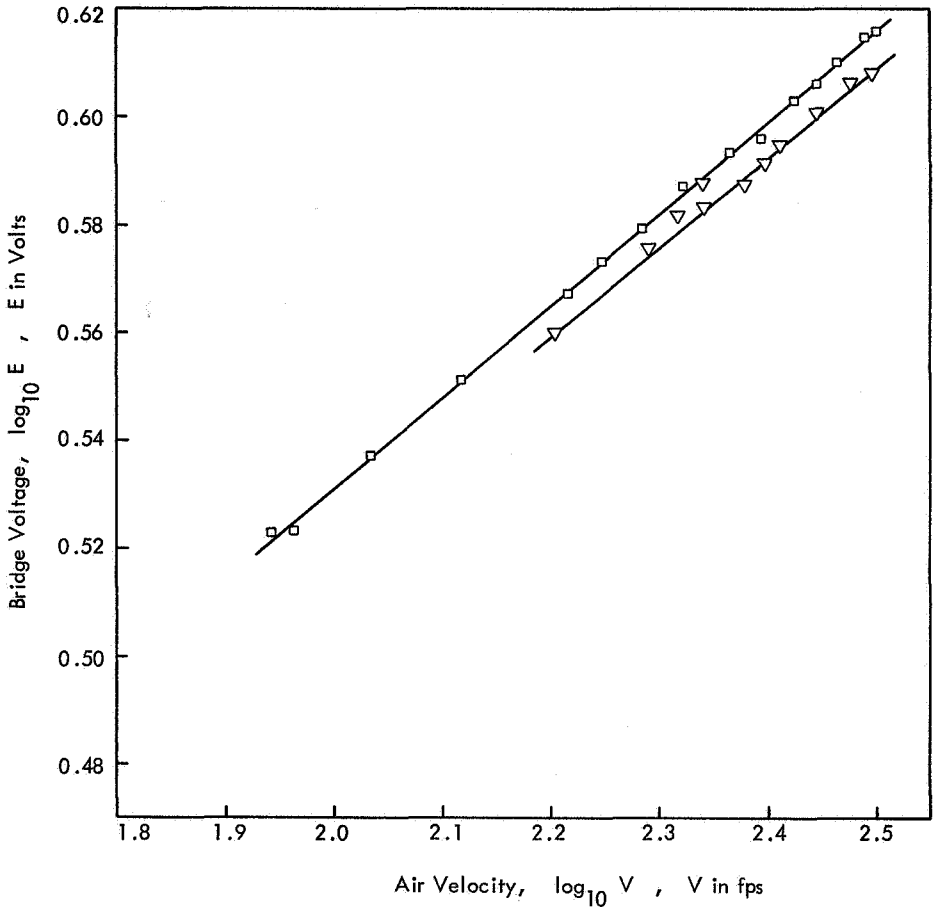


Figure 6b. Static Calibration of Wires, (log basis) (Concluded)

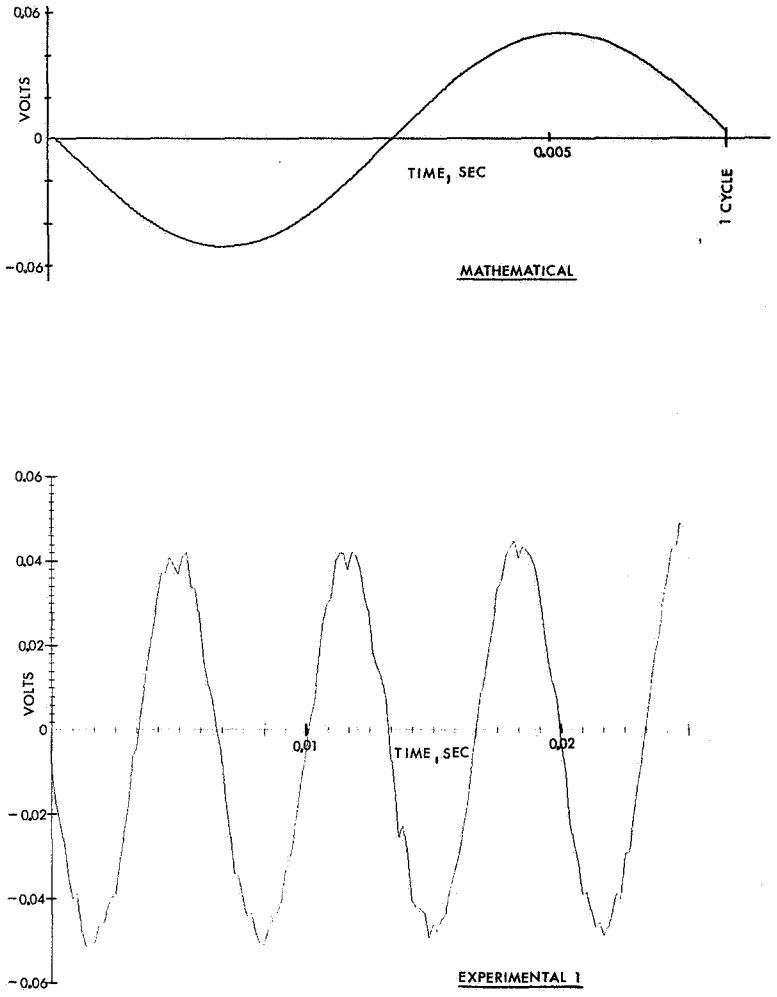


Figure 7. Run 7, Voltage Output for Experimental and Mathematical Results

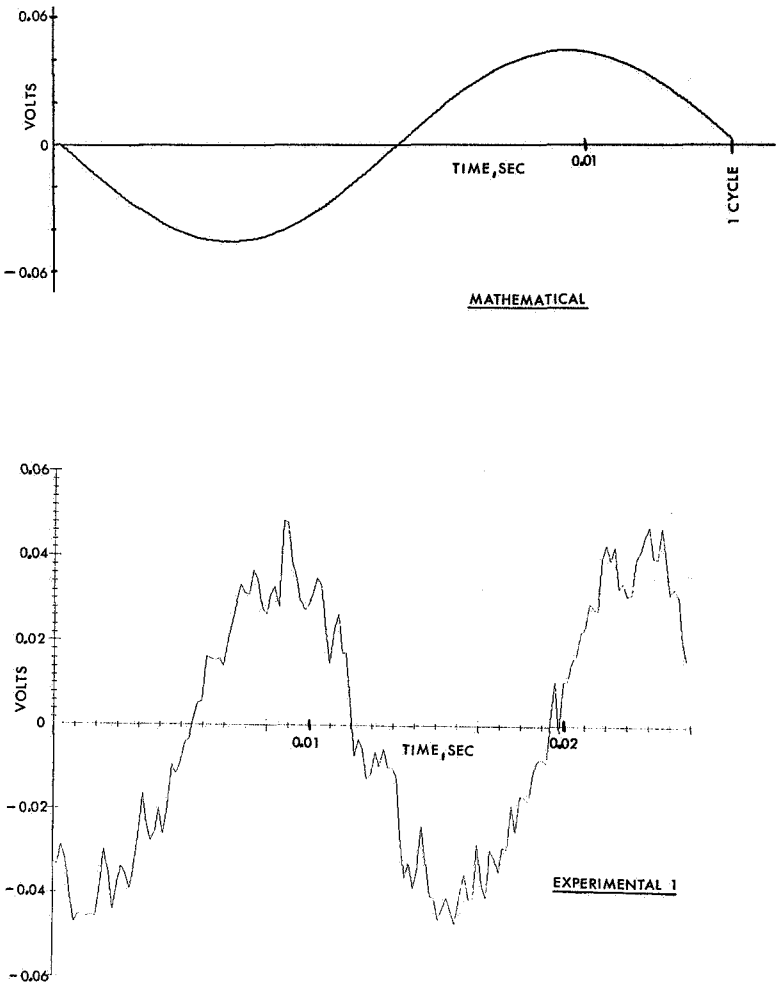


Figure 8. Run 5, Voltage Output for Experimental and Mathematical Results, Showing Turbulence in Air Flow

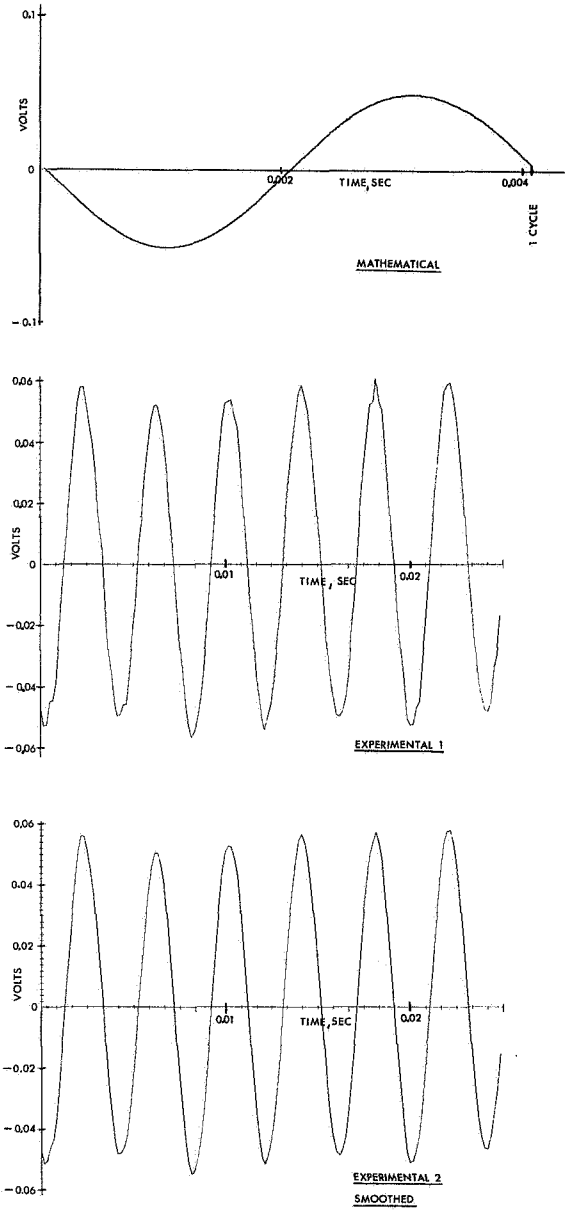


Figure 9. Run 11, Voltage Output Including Smoothing of Experimental Results

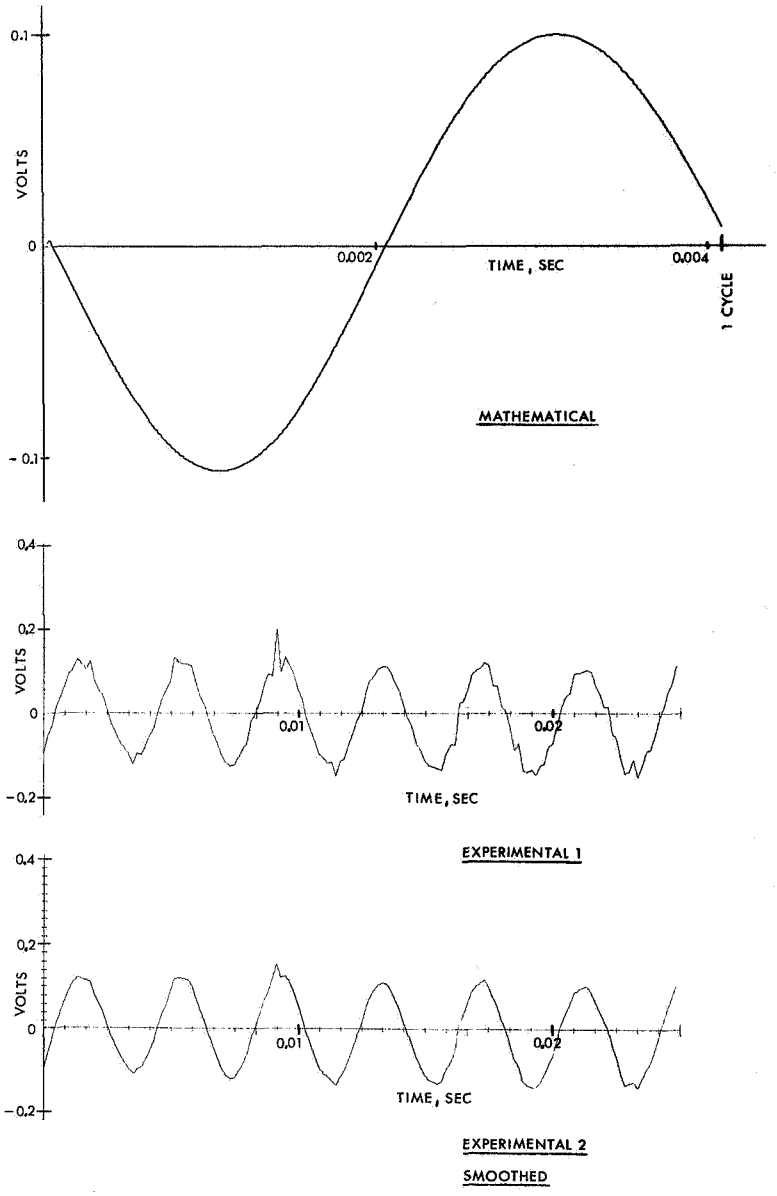


Figure 10. Run 15, Voltage Output Including Smoothing of Experimental Results

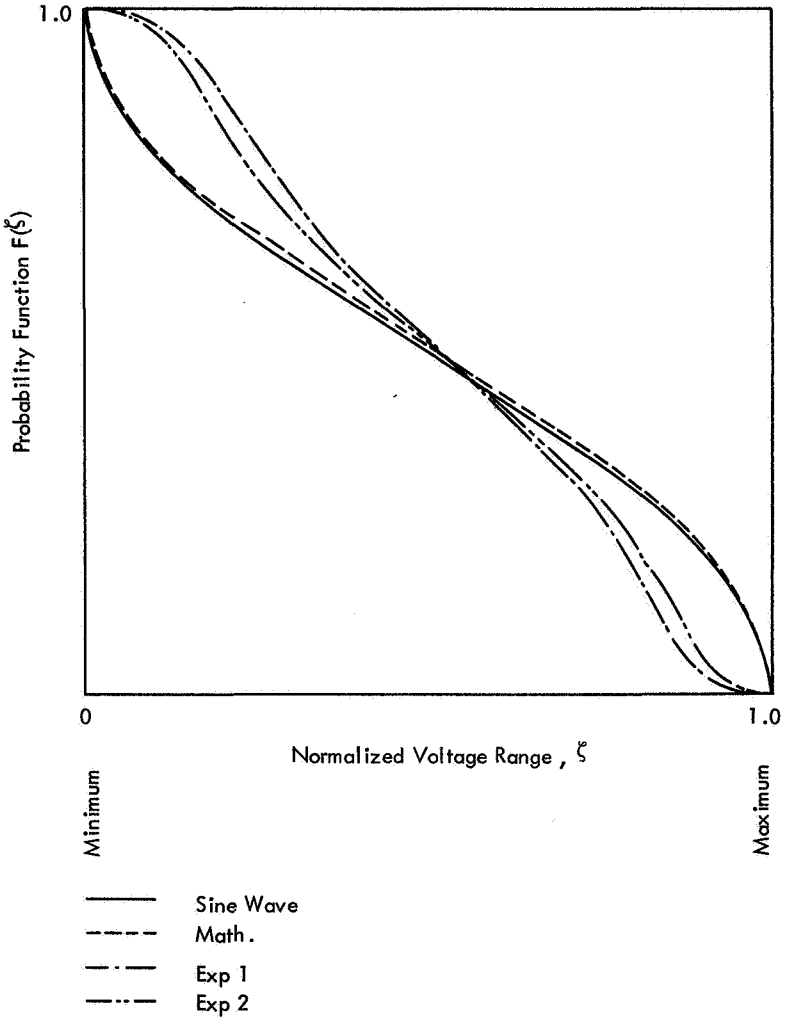


Figure 11. Run 2, Probability Functions of Signals

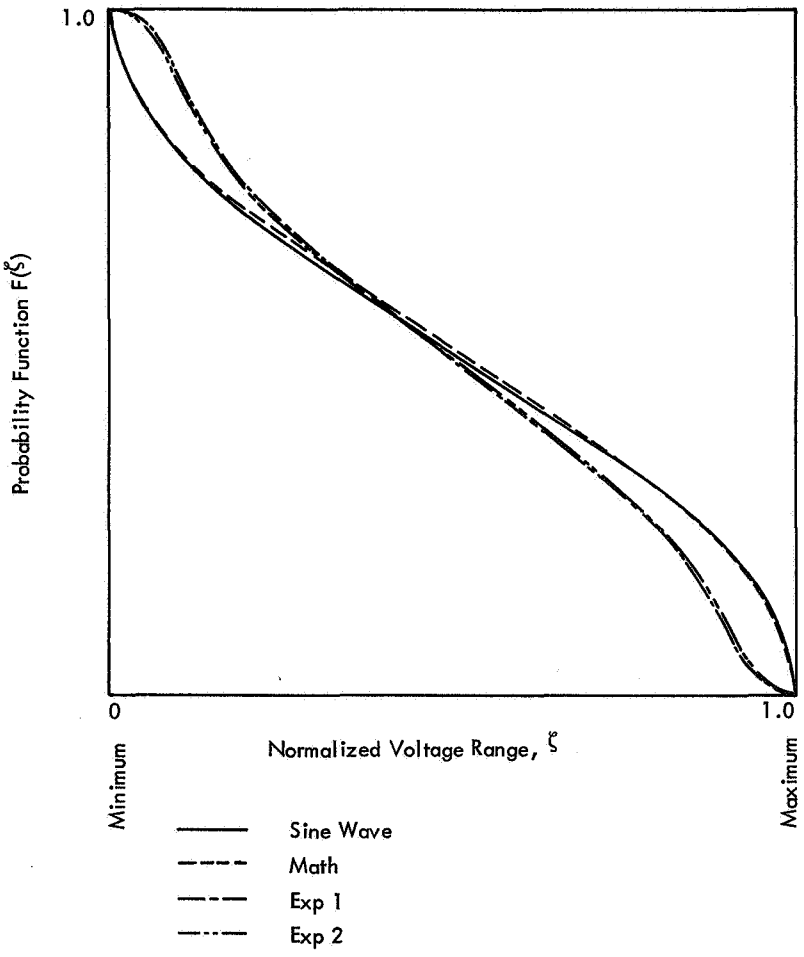


Figure 12. Run 8, Probability Functions of Signals

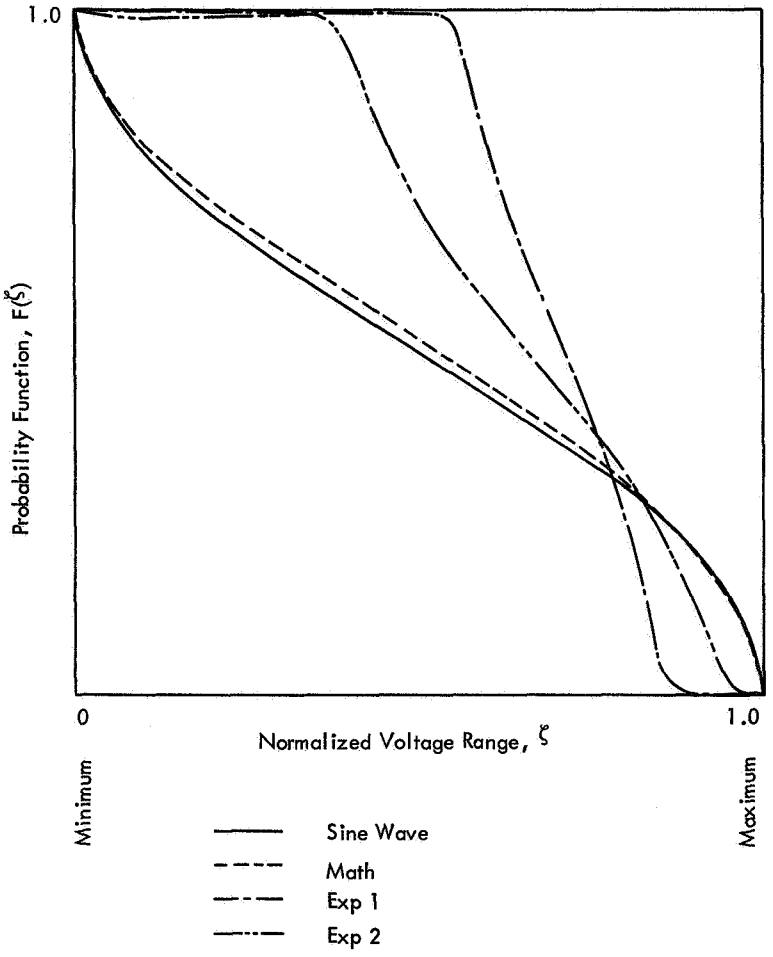


Figure 13. Run 15, Probability Functions of the Signals.

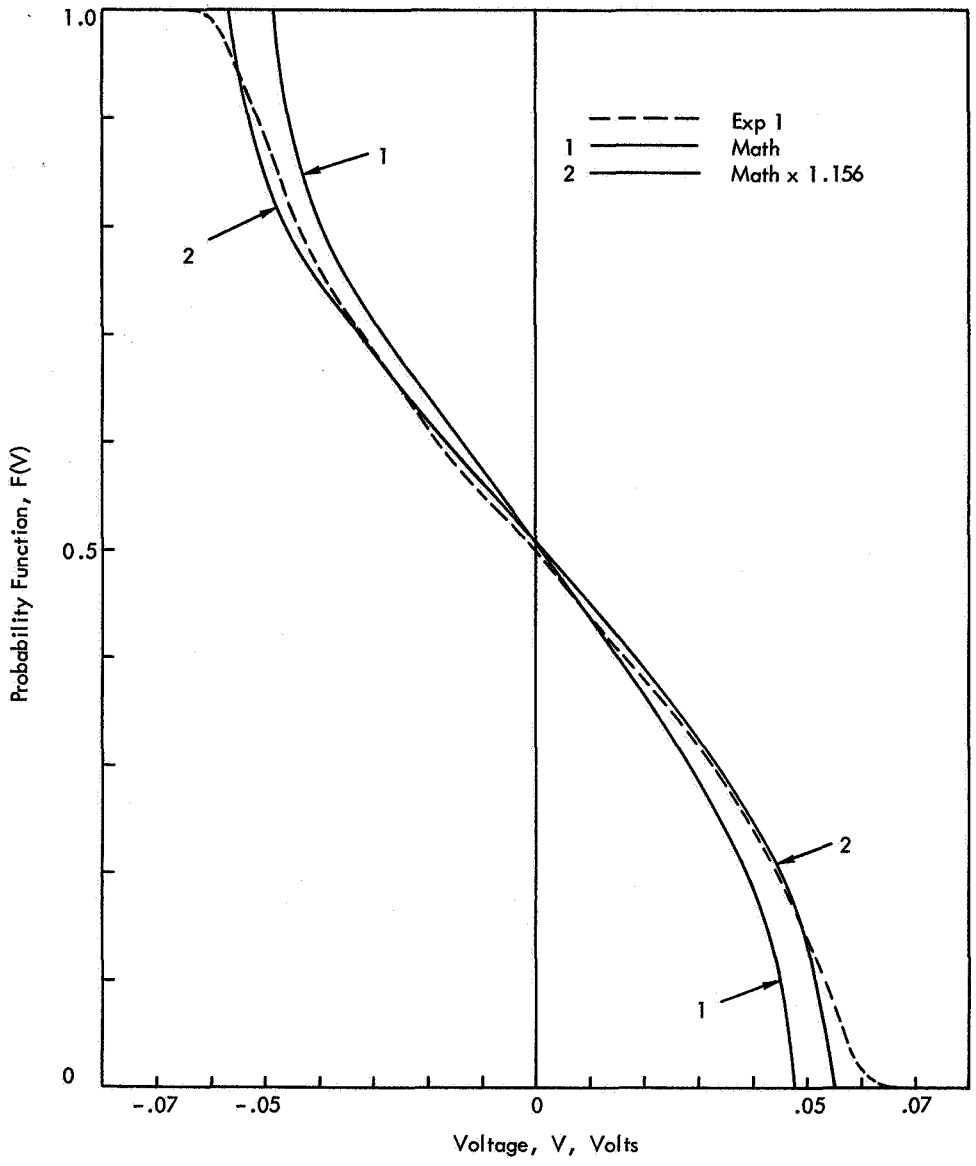


Figure 14. Run 8, Probability Function of Voltage

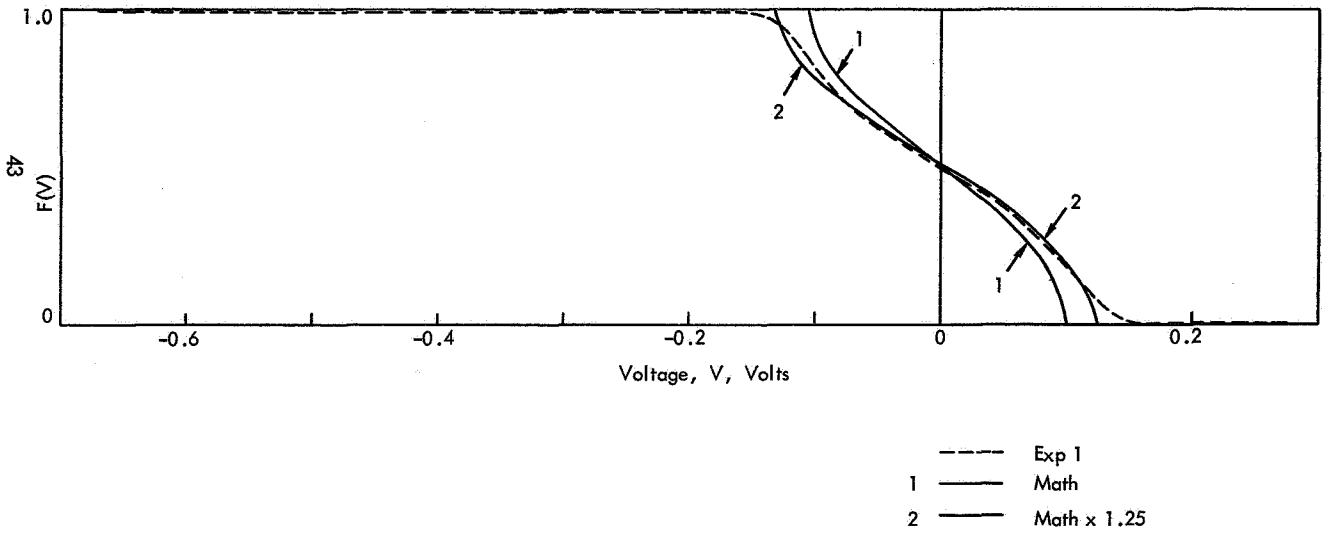


Figure 15: Run 15, Probability Function of Voltage

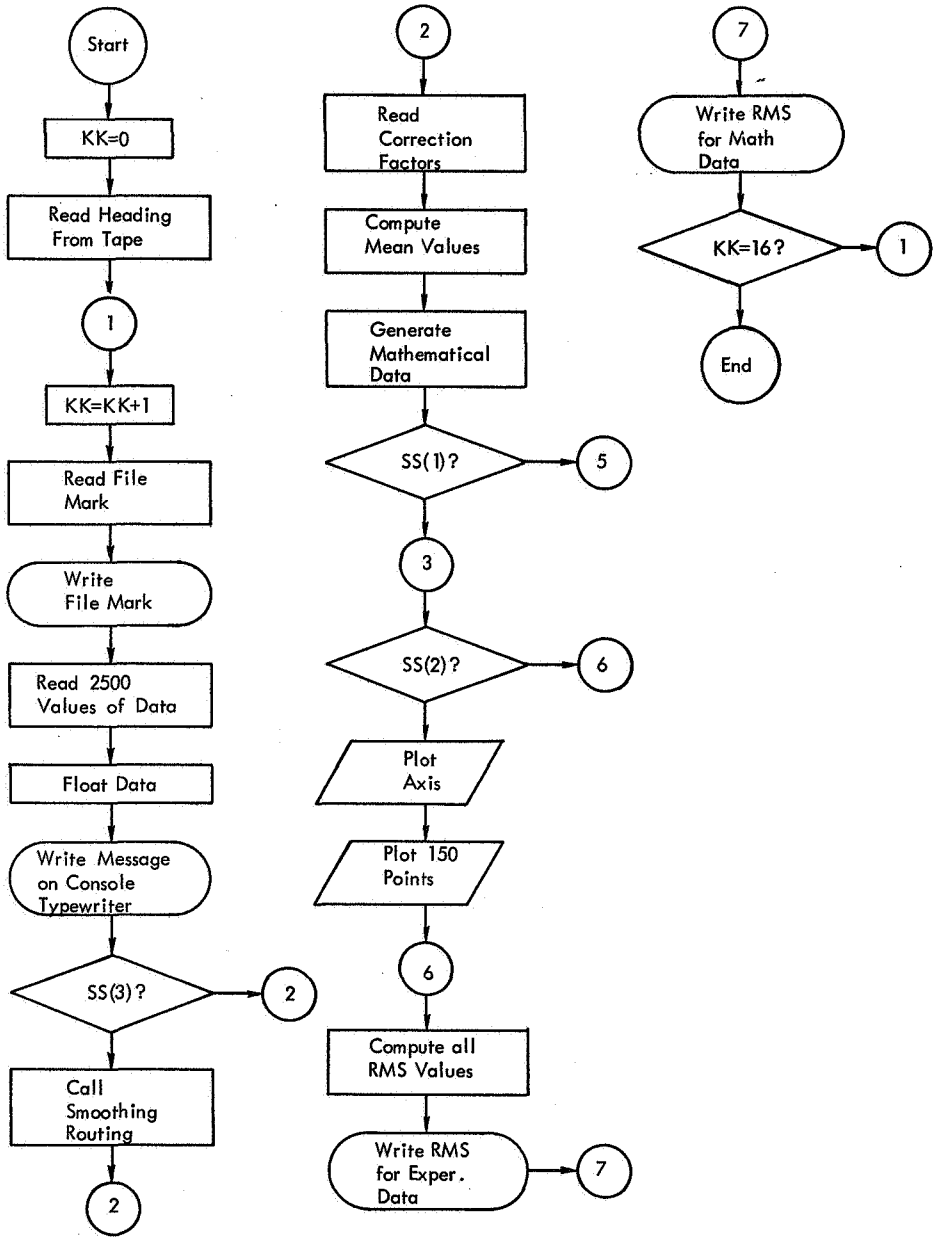


Figure 16: Flow Chart of Computer Program

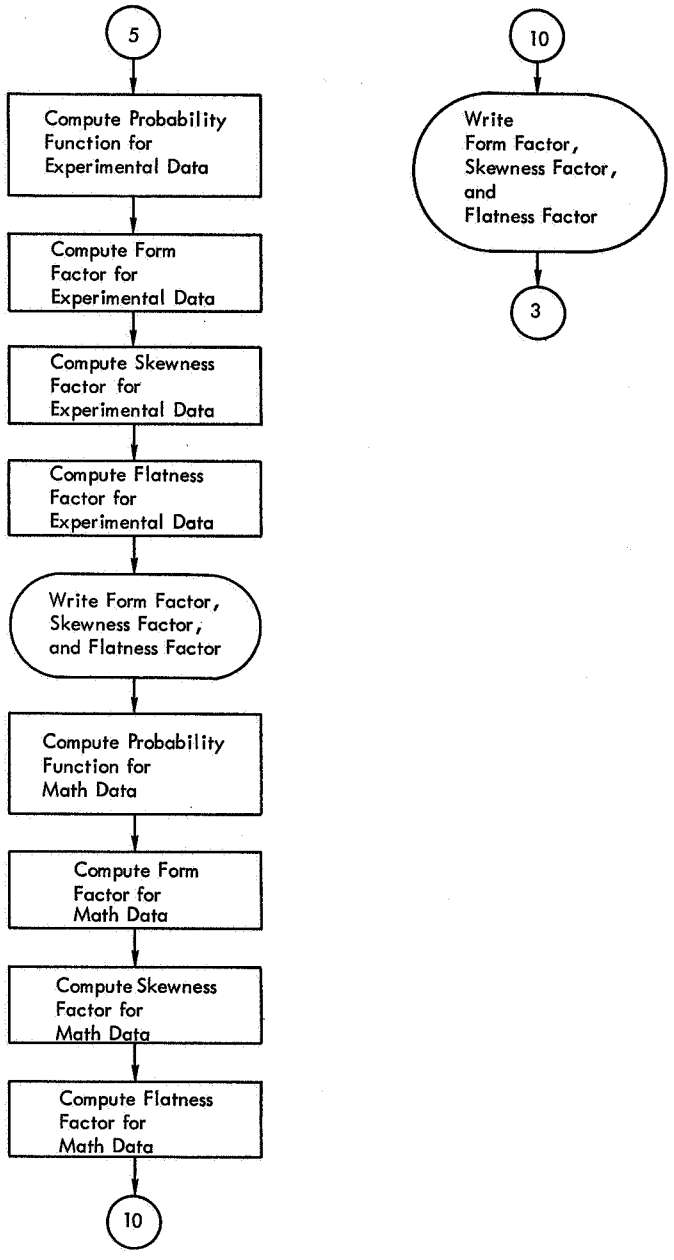


Figure 16: Flow Chart of Computer Program (Concluded)